Inorganic Chemistry

Article

pubs.acs.org/IC

What Factors Control O_2 Binding and Release Thermodynamics in Mononuclear Ruthenium Water Oxidation Catalysts? A Theoretical Exploration

Guiling Zhang,[†] Kejuan Chen,[†,‡] Hui Chen,*[,‡] Jiannian Yao,[‡] and Sason Shaik[§]

[†]Key Laboratory of Green Chemical Technology of College of Heilongjiang Province, College of Chemical and Environmental Engineering, Harbin University of Science and Technology, Harbin 150080, China

[‡]Beijing National Laboratory for Molecular Sciences (BNLMS), CAS Key Laboratory of Photochemistry, Institute of Chemistry, Chinese Academy of Sciences, Beijing 100190, China

[§]Institute of Chemistry and the Lise Meitner-Minerva Center for Computational Quantum Chemistry, The Hebrew University of Jerusalem, Givat Ram Campus, 91904 Jerusalem, Israel

Supporting Information

ABSTRACT: Mononuclear Ru-based water oxidation catalysts (WOCs) constitute an important class of WOCs for water splitting. This work constitutes a systematic study of Ru−O_2 complexes of mononuclear ruthenium WOCs, with a focus on the thermodynamics of water-assisted O_2 release in various electronic states and conformations. Our extensive DFT study reveals several factors that affect the O_2 release thermodynamics: (1) steric effect from the ligand sphere of Ru; (2) trans effect of ligands trans to O_2; (3) oxygen cis coordinating effect; (4) carbon coordinating effect; and (5) Ru coordination strength. Some of these effects could selectively stabilize/destabilize some states/conformations of the Ru−O_2 complexes relative to Ru−OH_2 complexes, and affect thereby the O_2 release thermodynamics. The identification and rationalization of factors for O_2 release thermodynamics, as in this work, could be helpful toward a better understanding of this final step of the ruthenium-catalyzed water oxidation.

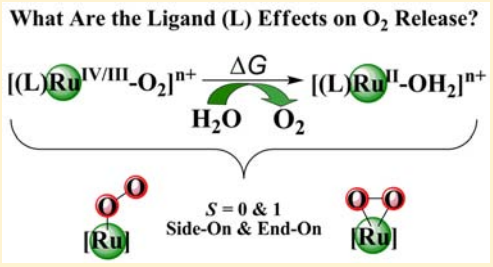

INTRODUCTION

Being highly demanding both thermodynamically and kinetically, the oxidation of water to produce oxygen is the most difficult step during water splitting. Nevertheless, the eventual control of this process is crucial for artificial photosynthesis aimed at solar energy usage,[1] and, therefore, the development of efficient water oxidation catalysts (WOCs) becomes essential. By far, the most extensively and thoroughly studied synthetic catalysts are ruthenium complexes.[2−9] The mononuclear ruthenium catalysts have attracted considerable interests due to their catalytic effectiveness and structural simplicity.[7−9] As such, they have become recurring targets for experimental and computational studies.[10−36] These studies have led to the following mechanistic proposal: The key O−O bond formation process involves either water nucleophilic attack (WNA) on Ru(V)═O to form Ru(III)−OOH or direct O−O coupling of two Ru(V)═O units (I2M) to form an O−O bridged dinuclear complex Ru(IV)−O−O−Ru(IV), which then releases O_2. To complete the catalytic cycle and regenerate the active high-valent Ru(V)═O species, various electron transfer and/or proton coupled electron transfer steps take place before and after O−O bond formation. Although this mechanistic scheme hypothesizes the generation of a RuO_2, direct experimental evidence for its existence is still rare.[24] Last but not least, the O_2 liberating process is essential for completion of the catalytic cycle. In some cases,[18,21,24,25,29] the O_2 release step has been implied experimentally to be the rate-limiting step during water oxidation by mononuclear ruthenium WOCs. Because of the complexity of the water oxidation process, its kinetics is affected by many experimental factors,[29,30] and, therefore, further experimental work is necessary to firmly establish the above mechanistic proposal and to clarify the situation. In addition, alternative mechanistic proposals with new features are often seen in the literature.[11,16,23,29]

Thus, despite the extensive experimental and theoretical studies on ruthenium-catalyzed water oxidation, our understanding of the factors that govern the O_2 release process is still limited. Especially, the influence of the Ru-supporting ligands (L) of the WOCs on the effectiveness of O_2 release from $[(L)RuO_2]^{n+}$ is not well-known. Even though there are case specific theoretical computations on some RuO_2 species,[16,19,21,23,24,31] to the best of our knowledge, there is still no systematic theoretical work to resolve this issue.

Received: December 31, 2012
Published: April 5, 2013

   dx.doi.org/10.1021/ic3028644 | Inorg. Chem. 2013, 52, 5088−5096

Scheme 1. Mononuclear Ruthenium Water Oxidation Catalysts Studied in This Work[a]

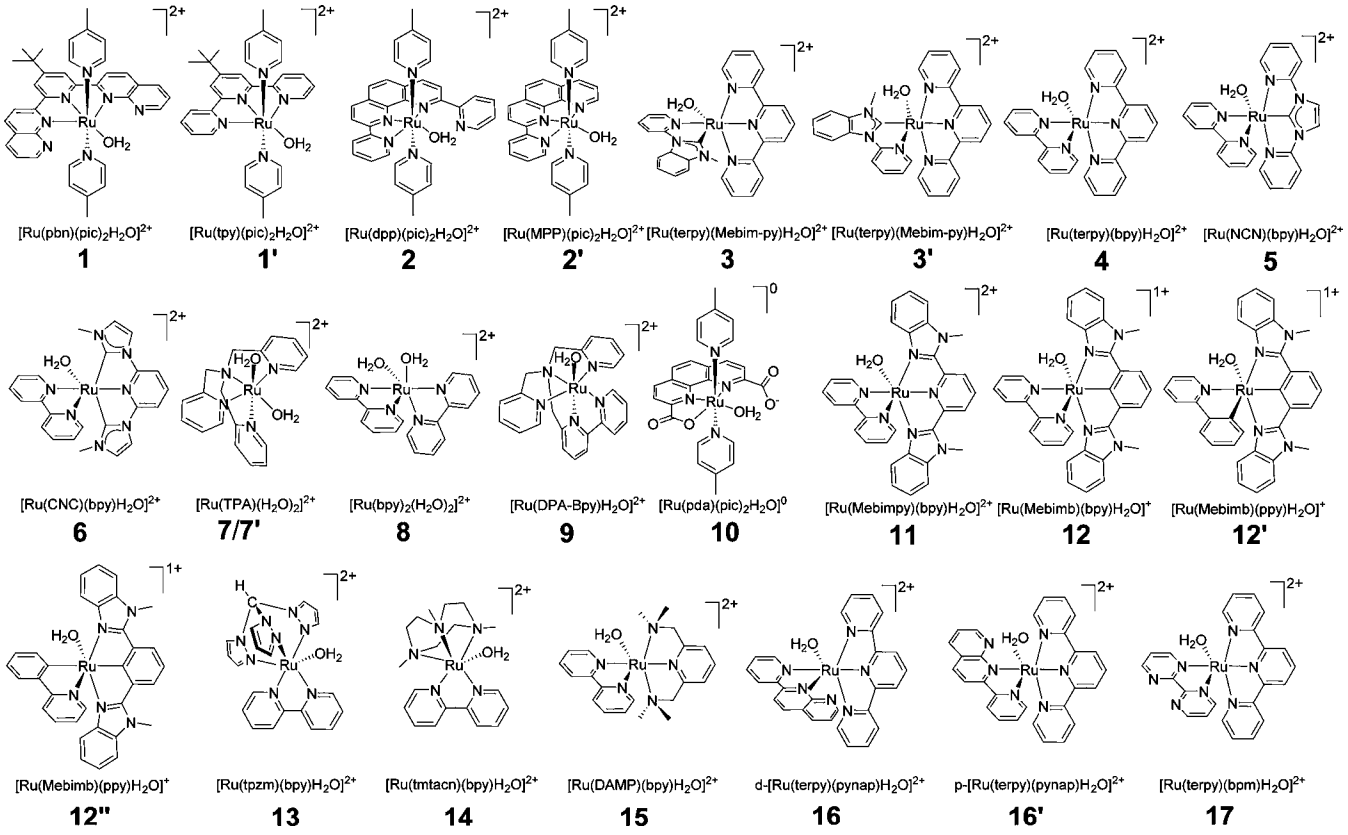

[a]The labels in bold below various WOCs denote their corresponding O_2-complexes, whose structures are generated from replacement of H_2O ligand by O_2 molecule. For 7/7′ case, whose WOC has two water ligands, 7 represents the amine-trans H_2O replaced structure, and 7′ represents the pyridine-trans H_2O replaced structure.

$$[(L)Ru^{IV/III} - O_2]^{n+} + H_2O \xrightarrow{\Delta G} [(L)Ru^{II} - OH_2]^{n+} + O_2 \quad (1)$$

On the basis of the Bell–Evans–Polanyi (BEP) principle,[37] the O_2 release reaction rate should correlate with the thermodynamics of O_2 release reaction. Thus, it would be very helpful to study the thermodynamics of the reaction to gain insight about the O_2 liberation from the catalyst. Herein, we explore and compare the thermodynamics of the O_2 release reaction from Ru(IV)-peroxo or Ru(III)-superoxo species assisted by water substitution (eq 1). This process is studied systematically for the mononuclear ruthenium WOCs depicted in Scheme 1, many of which are taken from previous experimental studies.[10,11,13−16,18,24,26a,27,35] We hope that this theoretical work can form a useful guide for researchers in the field of ruthenium WOCs when quick estimation of energetics in association with O_2 release process is necessary.

COMPUTATIONAL DETAILS

The structures of all species were optimized in the gas phase by PBE0 functional[38] using Ahlrichs' def-SVP[39] basis set. The PBE0 functional has been repeatedly found capable of producing very good geometries for transition metal (TM) complexes.[40−44] A vibrational analysis was carried out to confirm the optimized geometry is a true minimum with no imaginary frequency and to determine the thermal correction to Gibbs free energy. Single point calculations were performed with a large basis set, def2-TZVPP,[45] to refine the electronic energetics of these gas-phase-optimized minima using also a water solvent modeled by the SMD[46] continuum solvation model. Grimme's DFT-D3 empirical dispersion corrections were added to all of the energies reported in this work.[47] Free energies calculated herein include the solvation free energy in aqueous solution and thermal free energy correction in the gas phase at T = 298.15 K.

To identify low-energy electronic states, for the Ru–O_2 species, we calculated the four possible conformations/states combinations, which include closed-shell singlet states (O_2 side-on and end-on), and open-shell singlet state (O_2 end-on) and triplet state (O_2 end-on). Among these, the end-on closed-shell singlet state is much higher in energy than the corresponding end-on open-shell singlet state for all of the cases in Scheme 1 (see Table S1 in the Supporting Information). Thus, we shall not discuss this state further and relegated the corresponding results to the Supporting Information. Our test calculations on systems **1**–**17** (Scheme 1) indicated that the triplet side-on conformation is not a stable minimum, and it converts to triplet end-on conformation during geometry optimization. This result is in contrast to the recent DFT calculations on system **17** by Lin et al.,[21] for which the reason is still unclear.[48] The other structures in eq 1 like Ru(II)–OH_2, H_2O, and O_2 species were calculated in their ground states, that is, singlet, singlet, and triplet states, respectively.

Unrestricted DFT formalism was used for all open-shell calculations. Two hybrid density functionals, PBE0[38] and B3LYP,[49] were employed for single point calculation with the large basis set.[50] The two functionals generate similar results and trends, and hence we relegate the B3LYP results to the Supporting Information. All DFT calculations were carried out with the Gaussian 09 program.[51]

All open-shell singlet calculations for Ru–O_2 species were performed by broken-symmetry (BS) DFT approach to describe the BS singlet state with two unpaired electrons on Ru and O_2 moiety each. In such cases, Ru–O_2 singlet states could have large spin contamination. To address this issue, we adopted the Yamaguchi's

dx.doi.org/10.1021/ic3028644 | Inorg. Chem. 2013, 52, 5088−5096

Table 1. Electronic Energy (E) and Gibbs Free Energy (G) Changes (kcal/mol) of O_2 Release Shown in Equation 1 for All RuO_2 Complexes, and Their O−O Bond Lengths (R) (in Å)[a]

		ΔE			ΔG			R(O−O)		
label	complex[b]	$S_{side\text{-}on}$	$T_{end\text{-}on}$	$S_{end\text{-}on}$	$S_{side\text{-}on}$	$T_{end\text{-}on}$	$S_{end\text{-}on}$	$S_{side\text{-}on}$	$T_{end\text{-}on}$	$S_{end\text{-}on}$
1	Ru(pbn)(pic)$_2$(O_2)	−25.0	−17.4	−16.8	−25.0	**−15.0**	−16.5	1.33	1.19	1.24
1′	Ru(tpy)(pic)$_2$(O_2)	0.7	−7.9	−8.8	**−1.6**	−6.6	−8.3	1.33	1.21	1.23
2	Ru(dpp)(pic)$_2$(O_2)	−7.5	−12.6	−16.0	**−6.8**	−10.7	−15.1	1.33	1.21	1.22
2′	Ru(MPP)(pic)$_2$(O_2)	−0.5	−8.4	−11.2	**−2.2**	−6.3	−10.2	1.33	1.21	1.23
3	Ru(terpy)(Mebim-py)(O_2)	−9.0	−11.2	−22.4	−9.9	**−8.1**	−20.8	1.32	1.20	1.21
3′[c]	Ru(terpy)(Mebim-py)(O_2)	−7.8	−10.2	−8.4	−9.3	−9.3	**−6.4**	1.33	1.20	1.24
4	Ru(terpy)(bpy)(O_2)	−5.9	−10.4	−5.8	−6.7	−8.0	**−4.6**	1.33	1.20	1.24
5	Ru(NCN)(bpy)(O_2)	−6.1	−11.8	−2.5	−6.2	−8.9	**−1.4**	1.33	1.20	1.26
6	Ru(CNC)(bpy)(O_2)	−0.9	−9.9	−4.0	**−0.5**	−6.2	−2.6	1.34	1.20	1.24
7	Ru(TPA)(H_2O)(O_2)	4.2	−5.0	8.6	3.0	−4.7	**7.8**	1.33	1.21	1.27
7′[d]	Ru(TPA)(O_2)(H_2O)	−1.6	−5.9	3.0	−2.9	−3.5	**2.7**	1.33	1.21	1.27
8	Ru(bpy)$_2$(H_2O)(O_2)	−8.4	−10.3	−1.0	−9.3	−8.3	**−0.9**	1.32	1.20	1.26
9	Ru(DPA-Bpy)(O_2)	−0.3	−7.2	−11.4	**−1.6**	−5.1	−10.4	1.32	1.21	1.22
10	Ru(pda)(pic)$_2$(O_2)	−3.9	−16.4	−6.6	**−3.7**	−14.5	−5.2	1.33	1.26	1.26
11	Ru(Mebimpy)(bpy)(O_2)	−4.0	−9.7	0.2	−5.3	−7.5	**0.3**	1.33	1.21	1.26
12	Ru(Mebimb)(bpy)(O_2)	8.2	−2.6	10.8	6.8	−1.0	**11.1**	1.34	1.22	1.27
12′	Ru(Mebimb)(ppy)(O_2)	7.4	−3.1	0.7	**5.4**	−1.0	0.6	1.34	1.21	1.26
12″[e]	Ru(Mebimb)(ppy)(O_2)	6.9	−2.1	9.4	4.7	−1.0	**8.6**	1.34	1.22	1.27
13	Ru(tpzm)(bpy)(O_2)	−8.7	−10.9	−2.3	−9.7	−9.4	**−2.0**	1.32	1.20	1.26
14	Ru(tmtacn)(bpy)(O_2)	−3.1	−5.9	4.8	−4.0	−4.0	**5.1**	1.32	1.21	1.26
15	Ru(DAMP)(bpy)(O_2)	−6.6	−7.2	1.5	−8.5	−6.3	**1.1**	1.32	1.21	1.27
16	*d*-Ru(terpy)(pynap)(O_2)	−4.5	−11.3	−2.3	−5.3	−10.0	**−1.7**	1.33	1.21	1.26
16′	*p*-Ru(terpy)(pynap)(O_2)	−21.1	−18.5	−16.8	−20.7	−16.1	**−15.3**	1.31	1.20	1.25
17	Ru(terpy)(bpy)(O_2)	−8.6	−12.4	−8.9	−9.1	−10.9	**−7.5**	1.33	1.20	1.24

[a] $S_{side\text{-}on}$, $T_{end\text{-}on}$, and $S_{end\text{-}on}$ represent singlet side-on (closed-shell), triplet end-on (open-shell), and singlet end-on (open-shell) states, respectively. Negative energy means exothermic O_2 liberation. The energy change of O_2 liberation from the lowest free energy structure for each system is shown in bold. [b] Ligand abbreviations: pic = 4-picoline; pbn = 2,2′-(4-(*tert*-butyl)pyridine-2,6-diyl)bis(1,8-naphthyridine); tpy = 4′-*t*-butyl-2,2′:6′,2″-terpyridine; dpp = 2,9-di-(2′-pyridyl)-1,10-phenanthroline; terpy = 2,2′:6′,2″-terpyridine; Mebim-py = 3-methyl-1-pyridylbenzimidazol-2-ylidene; MPP = 2-(2-pyridyl)-1,10-phenanthroline; pda = 1,10-phenanthroline-2,9-dicarboxylic acid; bpy = 2,2′-bipyridine; tpzm = tris(1-pyrazolyl)methane; DPA-Bpy = *N*,*N*-bis(2-pyridinylmethyl)-2,2′-bipyridine-6-methanamine; NCN = 1,3-bis(pyridine-2-yl)imidazol-2-ylidene; CNC = 1,3-bis(1-methylbenzimidazol-2-yl)benzene; Mebimpy = 2,6-bis(1-methylbenzimidazol-2-yl)pyridine; DAMP = 2,6-bis(dimethylaminomethyl)pyridine; tmtacn = 1,4,7-trimethyl-1,4,7-triazacyclononane; TPA = tris(2-pyridylmethyl)amine; Mebimb = 2,6-bis(1-methylbenzimidazol-2-yl)benzene; ppy = 2-phenylpyridine; pynap = 2-(pyrid-2′-yl)-1,8-naphthyridine. [c] The most stable structure of **3′** ($S_{end\text{-}on}$) is 3.1 kcal/mol higher than **3** ($T_{end\text{-}on}$) in free energy. [d] The most stable structure of **7′** ($S_{end\text{-}on}$) is 5.0 kcal/mol higher than **7** ($S_{end\text{-}on}$) in free energy. [e] The most stable structure of **12″** ($S_{end\text{-}on}$) is 4.4 kcal/mol higher than **12′** ($S_{side\text{-}on}$) in free energy.

spin-projected correction[52] to compute the energy of the spin-purified low-spin (LS) state as:

$$ {}^{LS}E = \frac{{}^{BS}E\,{}^{HS}\langle S^2\rangle - {}^{HS}E\,{}^{BS}\langle S^2\rangle}{{}^{HS}\langle S^2\rangle - {}^{BS}\langle S^2\rangle} \quad (2) $$

Here, HS refers to the high-spin coupled state (triplet) that is related to the low-spin (LS) singlet state by spin flip, and $\langle S^2\rangle$ is the calculated spin expectation value of the spin-contaminated broken symmetry (BS) singlet state. More details on $\langle S^2\rangle$ and energies for these spin-projected corrections can be found in the Supporting Information.

RESULTS AND DISCUSSION

Table 1 summarizes the calculated electronic energy (ΔE) and Gibbs free energies (ΔG) for the water-assisted O_2 release reaction (eq 1) for all of the mononuclear ruthenium systems in Scheme 1. Also shown in the table are the O−O bond lengths in O_2 complexes. From the generally longer O−O bond lengths in side-on Ru−O_2 species than those in the corresponding end-on Ru−O_2 species, it is clear that side-on complexes resemble peroxo species more than the end-on ones. Naturally, this means the side-on RuO_2 complexes are associated with a greater oxidation number of the Ru as compared to the end-on ones. Concerning low-lying electronic structures of RuO2 complexes, the largest number of unpaired electrons on Ru is only one (in triplet and open-shell singlet). Thus generally, unlike its 3d TM congener FeO_2,[53] the tendency thereof to have multiple parallel unpaired electrons on TM center is quenched in RuO_2 complex, especially for side-on one with more saturated coordination sphere, wherein only closed-shell singlet state is obtained. This observation is consistent with the larger exchange interactions to stabilize multiple parallel unpaired electrons on TM center in Fe than in Ru, and the larger orbital-promotion gaps in 4d than in 3d TMs to disfavor multiple parallel unpaired electrons on TM center.[54]

Before we proceed with the energetic data in Table 1, it is informative to compare some of our computed energetics to the previous results. Polyansky, Fujita, and their co-workers had calculated the free energy difference between the side-on singlet and end-on triplet states of **1**,[16] and found a value of −13.2 kcal/mol in favor of the end-on triplet species. Our computed value of −10.0 kcal/mol is close to their value. Voorhis et al. reported the O_2 release thermodynamics of **17** from the triplet end-on RuO_2 conformation,[19] and their free energy value of −15.0 kcal/mol is reasonably close to our corresponding value of −10.9 kcal/mol. For **17**, Lin et al. computed the electronic energy gap between side-on singlet and open-shell end-on

dx.doi.org/10.1021/ic3028644 | Inorg. Chem. 2013, 52, 5088−5096

singlet states,[21] and found that the former state lies 2.1 kcal/mol below the latter. Our corresponding electronic energy gap value of 0.4 kcal/mol in favor of the side-on singlet state gives the same qualitative information. For **11**, Friesner et al. calculated the free energy gap between side-on singlet and end-on triplet states;[31] their value of 1.7 kcal/mol (side-on singlet higher in energy) and our value of −2.2 kcal/mol are reasonably close. Thus, generally, energetic results for RuO_2 species in this work are in accord with available previous theoretical results from other groups.[16,19,21,31]

Concerning the energy data in Table 1, first it can be seen that the free energy changes associated with the reaction from the lowest lying O_2-bound conformation (bold values in Table 1 for each system) span a range of 26.4 kcal/mol, from an exothermic process by −15.3 kcal/mol (**16′**) to an endothermic process by +11.1 kcal/mol (**12**). Second, the lowest-energy structures have mostly open-shell singlet states and Ru−O_2 end-on conformations. Only two cases (**1** and **3**) out of 24 have triplet Ru−O_2 end-on conformation as their lowest energy structure (for **1**, the singlet end-on conformation is just marginally higher than triplet end-on conformation). In seven of the cases (**1′**, **2**, **2′**, **6**, **9**, **10**, **12′**), the closed-shell side-on conformation is the lowest energy structure. Therefore, we may conclude that the O_2 release thermodynamics is dependent on: (1) steric effect from Ru ligands; (2) effect of ligand trans to O_2; (3) oxygen cis coordinating effect; (4) effect of carbon coordination; and (5) strength of the Ru coordination. Below, we analyze and discuss our results and elucidate the different factors affecting the thermodynamics of O_2 release.

Steric Effect. Steric repulsion is the first effect that is apparent in our thermodynamics data for O_2 release. As shown in Scheme 1, complex **1** differs from **1′** by having two additional fused pyridine rings attached to two side-coordinating pyridines of the terpyridine ligand. The resultant naphthyridine moieties could cause significantly larger steric hindrance for O_2 binding in **1** than in **1′**. This larger steric hindrance was demonstrated from Figure 1 in two equivalent ways:

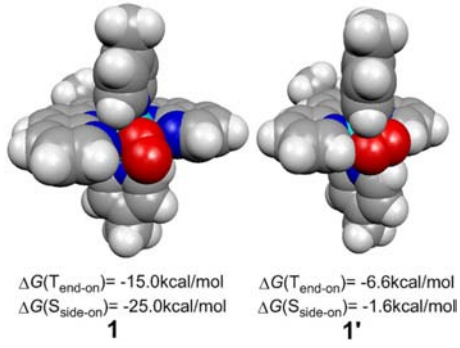

Figure 1. Space-filling models of the lowest energy structures of complexes **1** ($T_{end\text{-}on}$) and **1′** ($S_{side\text{-}on}$), and their O_2 release thermodynamics from $S_{side\text{-}on}$ and $T_{end\text{-}on}$ states.

(a) First, the two complexes **1** and **1′** show a large conformational energy difference between side-on and end-on conformations. **1** prefers an end-on conformation (triplet), which is 10.0 kcal/mol lower than the side-on structure, while on the contrary **1′** prefers a side-on structure, which is 5.0 kcal/mol lower than the lowest end-on complex (triplet). As shown in Figure 1, this conformational preference is due to the cleft generated by the naphthyridine moieties in **1**, which prefer an end-on O_2 coordination, as compared to the larger cleft in **1′**, which can accommodate O_2 in a side-on coordination.

(b) Second, the end-on and side-on conformations are quite different in the O_2 release thermodynamics difference between **1** and **1′**, which coincide with steric repulsion. Thus, comparing **1′** to **1**, one sees that the O_2 release from the more sterically encumbered side-on conformation is 23.4 kcal/mol less exothermic in **1′**. On the other hand, from the less encumbered end-on conformation (triplet), the O_2 release is only 8.4 kcal/mol less exothermic in **1′** versus **1**. This much larger change of O_2 release thermodynamics from **1** to **1′** in the side-on structures as compared to end-on structures is a manifestation of the large steric repulsion from the Ru ligands.

Additionally, it should be noted that as the product of O_2 release, the water coordinated complex of **1** has one H-bond (hydrogen bond) between H_2O and the N atom of the additional fused pyridine ring, as shown in Figure 2. This H-bond, which was also observed experimentally in the single-crystal X-ray structure,[13] is not present in **1′**. Thus, the H-bond in **1** stabilizes the water-coordinated complex, by several kcal/mol, thereby making O_2 release more exothermic in **1** than in **1′**. However, because this H-bond only effects a constant shift in the O_2 release thermodynamics for the side-on and end-on conformations of **1**, the O_2 release thermodynamics differences between **1** and **1′** for the side-on conformation (23.4 kcal/mol) and for the triplet end-on conformation (8.4 kcal/mol) as described above in point (b) are both equivalently affected by this H-bond. Hence, comparatively the difference in their differences (23.4 vs 8.4 kcal/mol, Figure 1) is still a manifestation of the steric hindrance difference between **1** and **1′**.

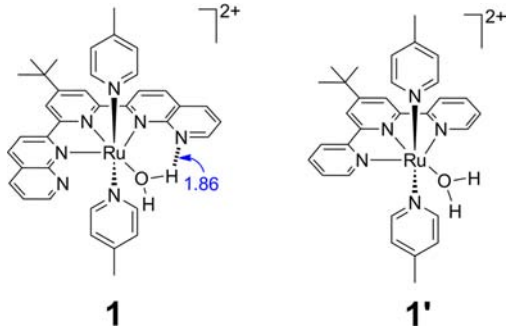

Figure 2. The structures (H-bond length labeled in Å) of the water complexes of **1** and **1′**.

1 has five possible coordinating nitrogen atoms in the equatorial ligand plane. This number is higher than the three nitrogens necessary for a usual octahedral coordination sphere of central Ru atom. These redundant coordinating positions are the root cause of the steric hindrance exerted by the ligand on O_2 binding. Inspection of **2** versus **2′** reveals that with 4-nitrogen sites in the equatorial plane of **2** the steric effects are small. Indeed, one finds the following facts from Figure 3: (a) **2** and **2′** do not show a large conformational energy difference between side-on and end-on conformations. Thus, for both **2** and **2′**, side-on conformation is lower in energy than the corresponding lowest end-on structure (triplet), by 3.9 and 4.1 kcal/mol, respectively. (b) The O_2 release thermodynamics

dx.doi.org/10.1021/ic3028644 | Inorg. Chem. 2013, 52, 5088−5096

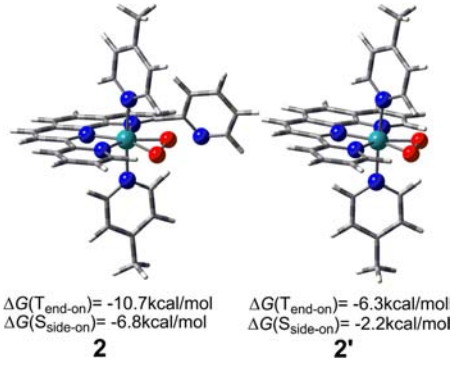

Figure 3. The lowest energy structures ($S_{side\text{-}on}$) of the complexes **2** and **2′**, and their O_2 release thermodynamics from $S_{side\text{-}on}$ and $T_{end\text{-}on}$ states.

differences between **2** and **2′** are similar from side-on (−4.6 kcal/mol) and lowest end-on (−4.4 kcal/mol) conformations. Thus, based on the comparison of **1** and **1′** above, **2** does not show apparent steric hindrance in comparison with **2′**. It should be noted that the 4.4−4.6 kcal/mol more exothermic O_2 release thermodynamics in **2** than in **2′** as shown in (b) originates from an H-bond between H_2O and one edge pyridine of equatorial ligand in the water coordinated complex of **2**, which is absent in the water complex of **2′** as shown in Figure 4. Thus, from the

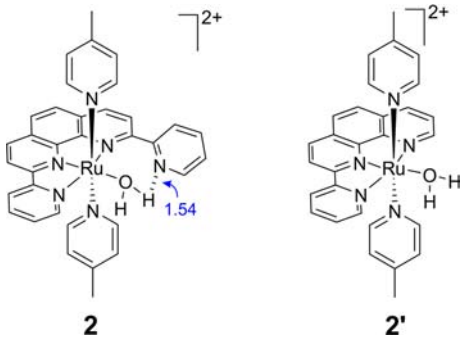

Figure 4. The structures (H-bond length labeled in Å) of the water complexes of **2** and **2′**.

above results, it appears that only those ligands that possess five or more equatorial coordinating sites can exert apparent steric hindrance effect to the O_2 bonding and releasing.

Another example of steric effect can be found from **16′**. As compared to **4**, the additional fused pyridine ring in the pynap ligand of **16′** exerts significant steric hindrance, as indicated by the much more exothermic O_2 release in the latter than the former. It is interesting to note that when fused pyridine ring in the pynap ligand is not in the vicinity of the O_2 coordinate site but far from it as in **16**, the steric hindrance is no longer present, and the O_2 release is much less exothermic than that of **16′**. Similar to **1** and **2**, the O_2 release thermodynamics for **16′** is also affected by the H-bond (Figure 5), between the coordinated water molecule, in the water complex, and the N atom of the fused pyridine ring in the pynap ligand. The calculated O---N distance, linked by the H-bond, is 2.60 Å, which is consistent with X-ray crystal structure data of 2.64−2.66 Å.[35] This distance match supports the presence of a H-bond in the water complex of **16′**.

From the above results, we see that the steric effect is a contributing factor for the thermodynamics of O_2 release in mononuclear ruthenium WOC. It is this effect that makes **1** and **16′** and exhibits the two most exothermic O_2 releases (−15.0 and −15.3 kcal/mol) among all of the cases in Table 1. Intramolecular hydrogen-bonding interaction of the water-coordinated complex could also play a role.

Trans Effect. The second factor found from our results is the trans effect exerted by the ligand in the trans position to O_2. The tighter is the binding/coordination (shorter bond length) of the ligand trans to O_2, the weaker will the O_2 binding be and vice versa. We can see this effect in **3** in Figure 5, which shows that **3** has N-heterocyclic carbene (NHC) coordinated trans to the O_2 binding site, and the Ru−C bond length is 1.99 Å, which is shorter than the corresponding Ru−N bond length of 2.09 Å in **4**. From Figure 5, we can see that this stronger Ru−C bonding in **3**, as compared to the Ru−N bond in **4**, exerts a strong and state-selective trans effect making the O_2 release thermodynamics, from the singlet end-on conformation, more exothermic by 16.2 kcal/mol as compared to **4** (−20.8 vs −4.6 kcal/mol), while there are only minor changes in the O_2 release thermodynamics of singlet side-on and triplet end-on states

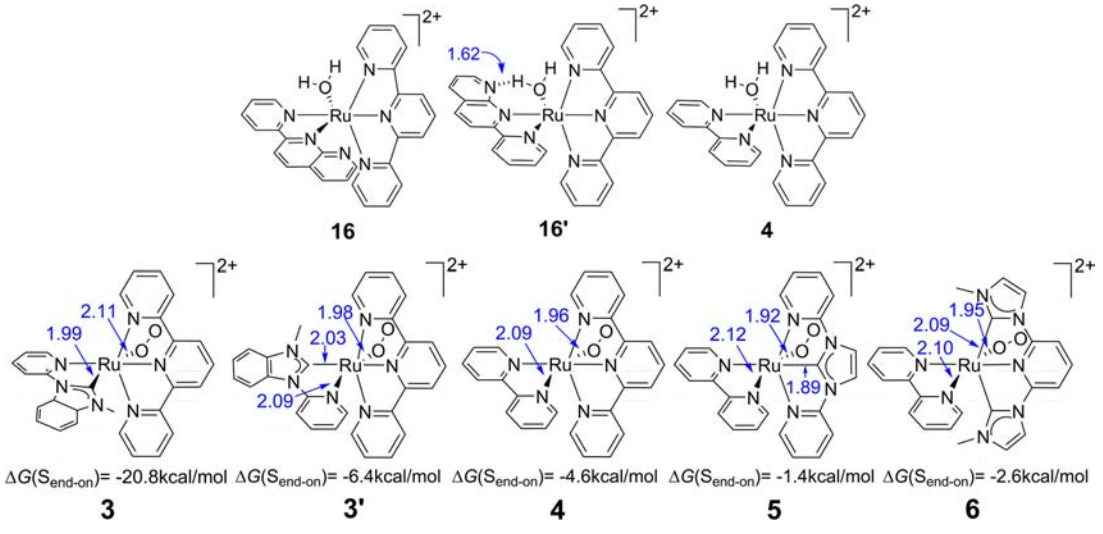

Figure 5. The structures (H-bond length labeled in Å) of the water complexes of **4**, **16**, and **16′**, and the structures (key bond lengths labeled in Å) and O_2 release thermodynamics of singlet end-on complexes of **3**, **3′**, **4**, **5**, and **6**.

dx.doi.org/10.1021/ic3028644 | Inorg. Chem. 2013, 52, 5088−5096

(see Table 1). This indicates a significant destabilization of the end-on O_2-binding in the singlet state relative to H_2O-binding or other forms of O_2 binding in the presence of *trans*-carbene ligand. Interestingly, when NHC coordinates in a cis position to O_2 as in **5** or **3′**, no large effect on O_2 release thermodynamics is observed in comparison with **4**. When two NHCs coordinate in two cis positions to O_2 as in **6**, there is also no apparent influence on the O_2 release thermodynamics.

Another example of the trans effect can be found in **7** and **7′** as depicted in Figure 6. The complexes differ by having

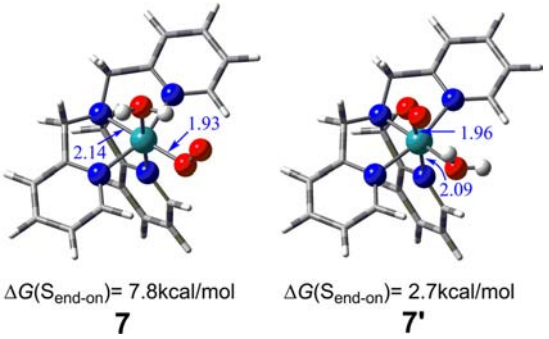

Figure 6. The lowest energy structures ($S_{end\text{-}on}$) of the complexes **7** and **7′** (key bond lengths labeled in Å), and their O_2 release thermodynamics.

different types of N atom coordination at the O_2 trans position, that is, an sp^3 aminic N atom in **7** versus an sp^2 pyridinic N atom in **7′**. The corresponding Ru−N bond length in **7** is 0.05 Å longer than **7′**, which originates from the sp^3 hybridized lone pair of the aminic N atom in the former, the sp^2 hybridized lone pair of pyridine N atom in the latter. Thus, the sp^2 hybridization in **7′** makes the N-ligand a more powerful donor, and hence its trans effect is more pronounced than in **7**, and the corresponding Ru−O_2 binding in **7′** is weaker. As shown in Figure 6, the O_2 release thermodynamics from the lowest singlet end-on conformation is indeed more favorable in **7′** by 5.1 kcal/mol.

Oxygen Coordinating Effect. In some of the complexes in Scheme 1, there are oxygen atoms coordinated at a cis position to O_2. These coordinated oxygen atoms belong either to water ligands (**7**, **7′**, **8**) or to a carboxylic group (**10**). We observed some uniform trend for these oxygen atom coordinated systems as compared to corresponding ones with all-nitrogen first coordinate sphere. As seen in Figure 7, when the edge pyridine of terpyridine ligand in **4** is replaced with water as in **8**, the O_2 release thermodynamics from the singlet end-on conformation becomes 3.7 kcal/mol less exothermic, while concurrently the O_2 release thermodynamics from singlet side-on conformation becomes 2.6 kcal/mol more exothermic. Thus, in the cis-oxygen ligated system **8**, the singlet end-on conformation is stabilized relative to the side-on conformation by 6.3 kcal/mol than that in all-nitrogen ligating complex **4**. Similar relative stabilizations of singlet end-on conformation over side-on one are also observed when changing from **9** to **7′**, and from **2** to **10**, which are of 14.4 and 6.8 kcal/mol, respectively.

Carbon Coordinating Effect. Except for the carbene complexes discussed above, aryl group coordination is also seen frequently in mononuclear ruthenium WOCs, as in **12**, **12′**, **12″** shown in Figure 8. In **12′**, C is at the trans position to O_2, while in **12** and **12″**, it is at the cis position to O_2. In comparison with **11**, which is an all-nitrogen ligating analogue complex,

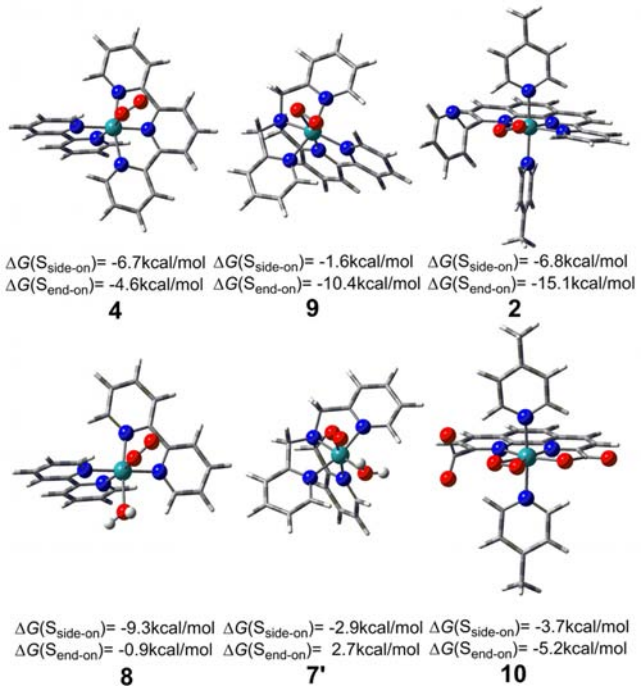

Figure 7. The lowest energy structures (key bond lengths labeled in Å) of the complexes **2** ($S_{side\text{-}on}$), **4** ($S_{end\text{-}on}$), **7′** ($S_{end\text{-}on}$), **8** ($S_{end\text{-}on}$), **9** ($S_{side\text{-}on}$), and **10** ($S_{side\text{-}on}$), and their O_2 release thermodynamics from $S_{side\text{-}on}$ and $S_{end\text{-}on}$ states.

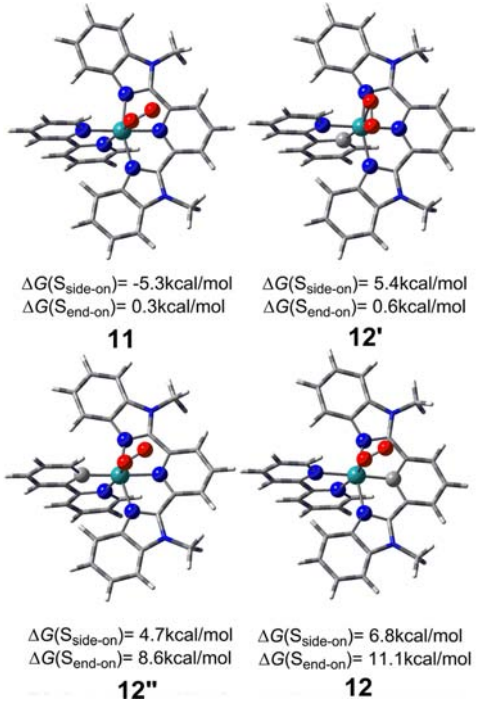

Figure 8. The lowest energy structures of the complexes **11** ($S_{end\text{-}on}$), **12** ($S_{end\text{-}on}$), **12′** ($S_{side\text{-}on}$), and **12″** ($S_{end\text{-}on}$), and their O_2 release thermodynamics from $S_{side\text{-}on}$ and $S_{end\text{-}on}$ states.

complexes **12**, **12′**, and **12″** exhibit different O_2 release thermodynamics. In **12′**, wherein C ligates at the trans position to O_2, the O_2 release thermodynamics become more endothermic than that in **11** by 10.7 and 6.5 kcal/mol from singlet side-on and triplet end-on conformations, respectively, while from singlet end-on conformation, the O_2 release

dx.doi.org/10.1021/ic3028644 | Inorg. Chem. 2013, 52, 5088−5096

thermodynamics almost does not change. Differently, in **12** and **12″**, wherein C ligates at the cis position of O_2, O_2 release thermodynamics from all three conformations (triplet end-on, singlet end-on, singlet side-on) change apparently toward the more endothermic direction. Thus, when aryl C ligates Ru, almost all conformations are significantly stabilized as compared to the all-nitrogen ligating complex. The only exception is the singlet end-on conformation, which is almost unaffected when C ligates at the trans position of O_2.

Ru Coordination Strength. We also observed some ligand effect due to different degrees of coordination by the same ligating atoms. As seen in Figure 9 and Table 2, the difference

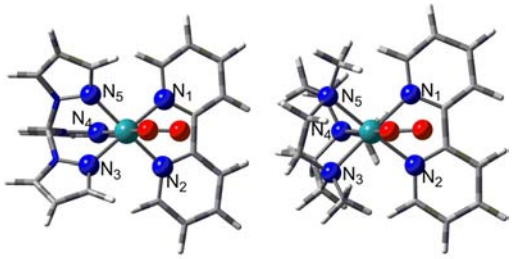

Figure 9. The singlet end-on structures of complexes **13** and **14**, and their O_2 release thermodynamics.

Table 2. Ru−N and Ru−O Bond Distances (in Å) of Complexes 13 and 14[a]

	13	14
Ru−N_1	2.07	2.12
Ru−N_2	2.07	2.14
Ru−N_3	2.10	2.19
Ru−N_4	2.03	2.12
Ru−N_5	2.10	2.18
Ru−O	2.04	2.02

[a]For N labeling, see Figure 9.

between sp^2 N-atom ligation of the pyrazol ring in **13** and the sp^3 N-atom ligation of the amine ligation in **14** leads to apparent different Ru−N bond lengths by about 0.1 Å. In the former complex, Ru−N is much shorter than that in the latter. Thus, the Ru center of **13** is coordinated more strongly than **14**, thereby making the O_2 release thermodynamics of **13** less endothermic than that of **14** (see also Table 1). The bond tightening in **13** is similar to the trans effect discussed above.

A similar observation about the effect of coordination strength applies to **4** versus **15**; the former has tighter bonds than the latter, as shown in Figure 10. Indeed, the O_2 release in **4** is −4.6 kcal/mol exothermic, whereas in **15** the same process is 1.1 kcal/mol endothermic.

CONCLUSIONS

This work constitutes a systematic study of the water-assisted O_2 release thermodynamics in various electronic states (singlet and triplet) and geometric conformations (side-on and end-on Ru−O_2 coordination) of Ru−O_2 complexes of mononuclear ruthenium water oxidation catalysts. The DFT calculations demonstrate that there are several factors that can affect the O_2 release thermodynamics: (1) steric effect from the ligand sphere of Ru; (2) a trans effect of ligand trans to O_2; (3) an

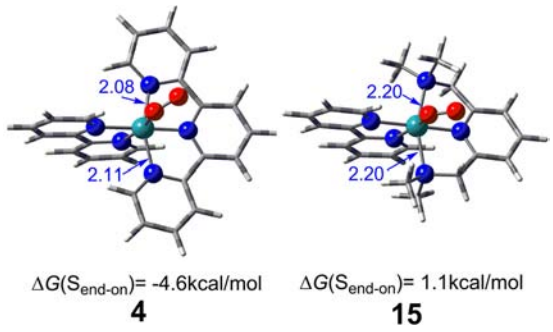

Figure 10. The singlet end-on structures (key bond lengths labeled in Å) of complexes **4** and **15**, and their O_2 release thermodynamics.

oxygen cis coordinating effect; (4) a carbon coordinating effect; and (5) a Ru coordination strength. Some of these effects could selectively stabilize/destabilize some states/conformations of the Ru−O_2 complexes relative to Ru−OH_2 complexes, and affect thereby the O_2 release thermodynamics.

The identification and rationalization of factors for O_2 release thermodynamics, which is closely related to the facility of O_2-liberation in water oxidation, could contribute to a better understanding of this final step in the cycle of water oxidation catalyzed by the ruthenium complexes.

ASSOCIATED CONTENT

Supporting Information

Three tables of computational results, and Cartesian coordinates of all species. This material is available free of charge via the Internet at http://pubs.acs.org.

AUTHOR INFORMATION

Corresponding Author

*E-mail: chenh@iccas.ac.cn.

Notes

The authors declare no competing financial interest.

ACKNOWLEDGMENTS

This work was supported by the Chinese Academy of Sciences and NSFC (Grants 21290194 and 51073048). S.S. acknowledges support by the ISF.

REFERENCES

(1) (a) Lewis, N. S.; Nocera, D. G. *Proc. Natl. Acad. Sci. U.S.A.* **2006**, *103*, 15729−15735. (b) Cook, T. R.; Dogutan, D. K.; Reece, S. Y.; Surendranath, Y.; Teets, T. S.; Nocera, D. G. *Chem. Rev.* **2010**, *110*, 6474−6502. (c) Balzani, V.; Credi, A.; Venturi, M. *ChemSusChem* **2008**, *1*, 26−58. (d) Armaroli, N.; Balzani, V. *Angew. Chem., Int. Ed.* **2007**, *46*, 52−66. (e) Gust, D.; Moore, T. A.; Moore, A. L. *Acc. Chem. Res.* **2009**, *42*, 1890−1898.

(2) (a) Rüttinger, W.; Dismukes, G. C. *Chem. Rev.* **1997**, *97*, 1−24. (b) Yagi, M.; Kaneko, M. *Chem. Rev.* **2001**, *101*, 21−35.

(3) (a) Sun, L. C.; Hammarström, L.; Åkermark, B.; Styring, S. *Chem. Soc. Rev.* **2001**, *30*, 36−49. (b) Lv, H. J.; Geletii, Y. V.; Zhao, C. C.; Vickers, J. W.; Zhu, G. B.; Luo, Z.; Song, J.; Lian, T. Q.; Musaev, D. G.; Hill, C. L. *Chem. Soc. Rev.* **2012**, *41*, 7572−7589.

(4) (a) Yamazaki, H.; Shouji, A.; Kajita, M.; Yagi, M. *Coord. Chem. Rev.* **2010**, *254*, 2483−2491. (b) Dau, H.; Limberg, C.; Reier, T.; Risch, M.; Roggan, S.; Strasser, P. *ChemCatChem* **2010**, *2*, 724−761. (c) Liu, X.; Wang, F. *Coord. Chem. Rev.* **2012**, *256*, 1115−1136. (d) Limburg, B.; Bouwman, E.; Bonnet, S. *Coord. Chem. Rev.* **2012**, *256*, 1451−1467.

(5) (a) Concepcion, J. J.; Jurss, J. W.; Brennaman, M. K.; Hoertz, P. G.; Patrocinio, A. O. T.; Iha, N. Y. M.; Templeton, J. L.; Meyer, T. J. *Acc. Chem. Res.* **2009**, *42*, 1954−1965. (b) Gagliardi, C. J.; Vannucci, A. K.; Concepcion, J. J.; Chen, Z.; Meyer, T. J. *Energy Environ. Sci.* **2012**, *5*, 7704−7717.
(6) Romain, S.; Vigara, L.; Llobet, A. *Acc. Chem. Res.* **2009**, *42*, 1944−1953.
(7) Cao, R.; Lai, W. Z.; Du, P. W. *Energy Environ. Sci.* **2012**, *5*, 8134−8157.
(8) Hetterscheid, D. G. H.; Reek, J. N. H. *Angew. Chem., Int. Ed.* **2012**, *51*, 9740−9747.
(9) Wasylenko, D. J.; Palmer, R. D.; Berlinguette, C. P. *Chem. Commun.* **2013**, *49*, 218−227.
(10) (a) Sala, X.; Ertem, M. Z.; Vigara, L.; Todorova, T. K.; Chen, W.; Rocha, R. C.; Aquilante, F.; Cramer, C. J.; Gagliardi, L.; Llobet, A. *Angew. Chem., Int. Ed.* **2010**, *49*, 7745−7747. (b) Vigara, L.; Ertem, M. Z.; Planas, N.; Bozoglian, F.; Leidel, N.; Dau, H.; Haumann, M.; Gagliardi, L.; Cramer, C. J.; Llobet, A. *Chem. Sci.* **2012**, *3*, 2576−2586.
(11) Yoshida, M.; Masaoka, S.; Abe, J.; Sakai, K. *Chem. Asian J.* **2010**, *5*, 2369−2378.
(12) Yoshida, M.; Masaoka, S.; Sakai, K. *Chem. Lett.* **2009**, *38*, 702−703.
(13) Zong, R.; Thummel, R. P. *J. Am. Chem. Soc.* **2005**, *127*, 12802−12803.
(14) Zhang, G.; Zong, R.; Tseng, H.-W.; Thummel, R. P. *Inorg. Chem.* **2008**, *47*, 990−998.
(15) Radaram, B.; Ivie, J. A.; Singh, W. M.; Grudzien, R. M.; Reibenspies, J. H.; Webster, C. E.; Zhao, X. *Inorg. Chem.* **2011**, *50*, 10564−10571.
(16) Polyansky, D. E.; Muckerman, J. T.; Rochford, J.; Zong, R.; Thummel, R. P.; Fujita, E. *J. Am. Chem. Soc.* **2011**, *133*, 14649−14665.
(17) Tseng, H.-W.; Zong, R.; Muckerman, J. T.; Thummel, R. P. *Inorg. Chem.* **2008**, *47*, 11763−11773.
(18) Concepcion, J. J.; Jurss, J. W.; Norris, M. R.; Chen, Z.; Templeton, J. L.; Meyer, T. J. *Inorg. Chem.* **2010**, *49*, 1277−1279.
(19) Wang, L.-P.; Wu, Q.; Voorhis, T. V. *Inorg. Chem.* **2010**, *49*, 4543−4553.
(20) Chen, Z.; Concepcion, J. J.; Hu, X.; Yang, W.; Hoertz, P. G.; Meyer, T. J. *Proc. Natl. Acad. Sci. U.S.A.* **2010**, *107*, 7225−7229.
(21) Lin, X. S.; Hu, X. Q.; Concepcion, J. J.; Chen, Z.; Liu, S. B.; Meyer, T. J.; Yang, W. *Proc. Natl. Acad. Sci. U.S.A.* **2012**, *109*, 15669−15672.
(22) Romero, I.; Rodríguez, M.; Sens, C.; Mola, J.; Kollipara, M. R.; Francàs, L.; Mas-Marza, E.; Escriche, L.; Llobet, A. *Inorg. Chem.* **2008**, *47*, 1824−1834.
(23) Kimoto, A.; Yamauchi, K.; Yoshida, M.; Masaoka, S.; Sakai, K. *Chem. Commun.* **2012**, *48*, 239−241.
(24) Concepcion, J. J.; Tsai, M.-K.; Muckerman, J. T.; Meyer, T. J. *J. Am. Chem. Soc.* **2010**, *132*, 1545−1557.
(25) Concepcion, J. J.; Jurss, J. W.; Templeton, J. L.; Meyer, T. J. *J. Am. Chem. Soc.* **2008**, *130*, 16462−16463.
(26) (a) Tong, L.; Duan, L.; Xu, Y.; Privalov, T.; Sun, L. C. *Angew. Chem., Int. Ed.* **2011**, *50*, 445−449. (b) Duan, L. L.; Bozoglian, F.; Mandal, S.; Stewart, B.; Privalov, T.; Llobet, A.; Sun, L. C. *Nat. Chem.* **2012**, *4*, 418−423. (c) Wang, L.; Duan, L. L.; Stewart, B.; Pu, M. P.; Liu, J. H.; Privalov, T.; Sun, L. C. *J. Am. Chem. Soc.* **2012**, *134*, 18868−18880. (d) Privalov, T.; kermark, B.; Sun, L. C. *Chem.-Eur. J.* **2011**, *17*, 8313−8317. (e) Nyhlén, J.; Duan, L. L.; Åkermark, B.; Sun, L. C.; Privalov, T. *Angew. Chem., Int. Ed.* **2010**, *49*, 1773−1777. (f) An, J. X.; Duan, L. L.; Sun, L. C. *Faraday Discuss.* **2012**, *155*, 267−275.
(27) Chen, Z.; Concepcion, J. J.; Meyer, T. J. *Dalton Trans.* **2011**, *40*, 3789−3792.
(28) Lai, W. Z.; Cao, R.; Dong, G.; Shaik, S.; Yao, J. N.; Chen, H. *J. Phys. Chem. Lett.* **2012**, *3*, 2315−2319.
(29) Wasylenko, D. J.; Ganesamoorthy, C.; Henderson, M. A.; Koivisto, B. D.; Osthoff, H. D.; Berlinguette, C. P. *J. Am. Chem. Soc.* **2010**, *132*, 16094−16106.
(30) Wasylenko, D. J.; Ganesamoorthy, C.; Henderson, M. A.; Berlinguette, C. P. *Inorg. Chem.* **2011**, *50*, 3662−3672.
(31) Hughes, T. F.; Friesner, R. A. *J. Phys. Chem. B* **2011**, *115*, 9280−9289.
(32) Chen, Y.; Fang, W. H. *J. Phys. Chem. A* **2010**, *114*, 10334−10338.
(33) Yang, X. Z.; Hall, M. B. *J. Am. Chem. Soc.* **2010**, *132*, 120−130.
(34) Vallés-Pardo, J. L.; Guijt, M. C.; Iannuzzi, M.; Joya, K. S.; de Groot, H. J. M.; Buda, F. *ChemPhysChem* **2012**, *13*, 140−146.
(35) (a) Yamazaki, H.; Hakamata, T.; Komi, M.; Yagi, M. *J. Am. Chem. Soc.* **2011**, *133*, 8846−8849. (b) Boyer, J. L.; Polyansky, D. E.; Szalda, D. J.; Zong, R. F.; Thummel, R. P.; Fujita, E. *Angew. Chem., Int. Ed.* **2011**, *50*, 12600−12604.
(36) Murakami, M.; Hong, D. C.; Suenobu, T.; Yamaguchi, S.; Ogura, T.; Fukuzumi, S. *J. Am. Chem. Soc.* **2011**, *133*, 11605−11613.
(37) (a) Bell, R. P. *Proc. R. Soc. London, Ser. A* **1936**, *154*, 414−421. (b) Evans, M. G.; Polanyi, M. *Trans. Faraday Soc.* **1938**, *34*, 11−24.
(38) (a) Perdew, J. P.; Burke, K.; Ernzerhof, M. *Phys. Rev. Lett.* **1996**, *77*, 3865−3868. (b) Ernzerhof, M.; Scuseria, G. E. *J. Chem. Phys.* **1999**, *110*, 5029−5036. (c) Adamo, C.; Barone, V. *J. Chem. Phys.* **1999**, *110*, 6158−6170.
(39) Schäfer, A.; Horn, H.; Ahlrichs, R. *J. Chem. Phys.* **1992**, *97*, 2571−2577.
(40) Kang, R. H.; Chen, H.; Shaik, S.; Yao, J. N. *J. Chem. Theory Comput.* **2011**, *7*, 4002−4011.
(41) (a) Bühl, M.; Reimann, C.; Pantazis, D. A.; Bredow, T.; Neese, F. *J. Chem. Theory Comput.* **2008**, *4*, 1449−1459. (b) Waller, M. P.; Braun, H.; Hojdis, N.; Bühl, M. *J. Chem. Theory Comput.* **2007**, *3*, 2234−2242. (c) Bühl, M.; Kabrede, H. *J. Chem. Theory Comput.* **2006**, *2*, 1282−1290.
(42) (a) Pierloot, K.; Vancoillie, S. *J. Chem. Phys.* **2006**, *125*, 124303. (b) Pierloot, K.; Vancoillie, S. *J. Chem. Phys.* **2008**, *128*, 034104. (c) Phung, Q. M.; Vancoillie, S.; Pierloot, K. *J. Chem. Theory Comput.* **2012**, *8*, 883−892.
(43) Zhao, S.; Li, Z. H.; Wang, W. N.; Liu, Z. P.; Fan, K. N.; Xie, Y. M.; Schaefer, H. F. *J. Chem. Phys.* **2006**, *124*, 184102.
(44) Kim, J.; Ihee, H.; Lee, Y. S. *J. Chem. Phys.* **2010**, *133*, 144309.
(45) Weigend, F.; Ahlrichs, R. *Phys. Chem. Chem. Phys.* **2005**, *7*, 3297−3305.
(46) Marenich, A. V.; Cramer, C. J.; Truhlar, D. G. *J. Phys. Chem. B* **2009**, *113*, 6378−6396.
(47) Grimme, S.; Antony, J.; Ehrlich, S.; Krieg, H. *J. Chem. Phys.* **2010**, *132*, 154104.
(48) We tested several factors in geometry optimization for triplet side-on conformation of **17**, including optimization in solvent (water) using continuum solvation model and different functionals (B3LYP and PBE0). However, we always find that the triplet side-on conformation changes to the triplet end-on structure during the geometry optimization. We note that such triplet side-on conformation was reported only in ref 21 but not seen in other theoretical studies dealing with RuO_2 species like refs 16, 19, 23, 24, 31.
(49) (a) Becke, A. D. *Phys. Rev. A* **1988**, *38*, 3098−3100. (b) Lee, C.; Yang, W.; Parr, R. G. *Phys. Rev. B* **1988**, *37*, 785−789. (c) Becke, A. D. *J. Chem. Phys.* **1993**, *98*, 5648−5652.
(50) For a recent ab initio assessment of DFT performance in the whole catalytic cycle of mononuclear Ru-WOC, see: Kang, R. H.; Yao, J. N.; Chen, H. *J. Chem. Theory Comput.* **2013**, *9*, 1872−1879.
(51) Frisch, M. J.; Trucks, G. W.; Schlegel, H. B.; Scuseria, G. E.; Robb, M. A.; Cheeseman, J. R.; Scalmani, G.; Barone, V.; Mennucci, B.; Petersson, G. A.; Nakatsuji, H.; Caricato, M.; Li, X.; Hratchian, H. P.; Izmaylov, A. F.; Bloino, J.; Zheng, G.; Sonnenberg, J. L.; Hada, M.; Ehara, M.; Toyota, K.; Fukuda, R.; Hasegawa, J.; Ishida, M.; Nakajima, T.; Honda, Y.; Kitao, O.; Nakai, H.; Vreven, T.; Montgomery, J. A., Jr.; Peralta, J. E.; Ogliaro, F.; Bearpark, M.; Heyd, J. J.; Brothers, E.; Kudin, K. N.; Staroverov, V. N.; Kobayashi, R.; Normand, J.; Raghavachari, K.; Rendell, A.; Burant, J. C.; Iyengar, S. S; Tomasi, J.; Cossi, M.; Rega, N.; Millam, J. M.; Klene, M.; Knox, J. E.; Cross, J. B.; Bakken, V.; Adamo, C.; Jaramillo, J.; Gomperts, R.; Stratmann, R. E.; Yazyev, O.; Austin, A. J.; Cammi, R.; Pomelli, C.; Ochterski, J. W.; Martin, R. L.; Morokuma, K.; Zakrzewski, V. G.; Voth, G. A.; Salvador, P.; Dannenberg, J. J.; Dapprich, S.; Daniels, A. D.; Farkas, O.; Foresman, J. B.; Ortiz, J. V.;

Cioslowski, J.; Fox, D. J. *Gaussian 09*, revision C.01; Gaussian, Inc.: Wallingford, CT, 2009.
(52) Yamaguchi, K.; Jensen, F.; Dorigo, A.; Houk, K. N. *Chem. Phys. Lett.* **1988**, *149*, 537.
(53) Chen, H.; Cho, K.-B.; Lai, W. Z.; Nam, W.; Shaik, S. *J. Chem. Theory Comput.* **2012**, *8*, 915−926.
(54) Shaik, S.; Chen, H.; Janardanan, D. *Nat. Chem.* **2011**, *3*, 19−27.